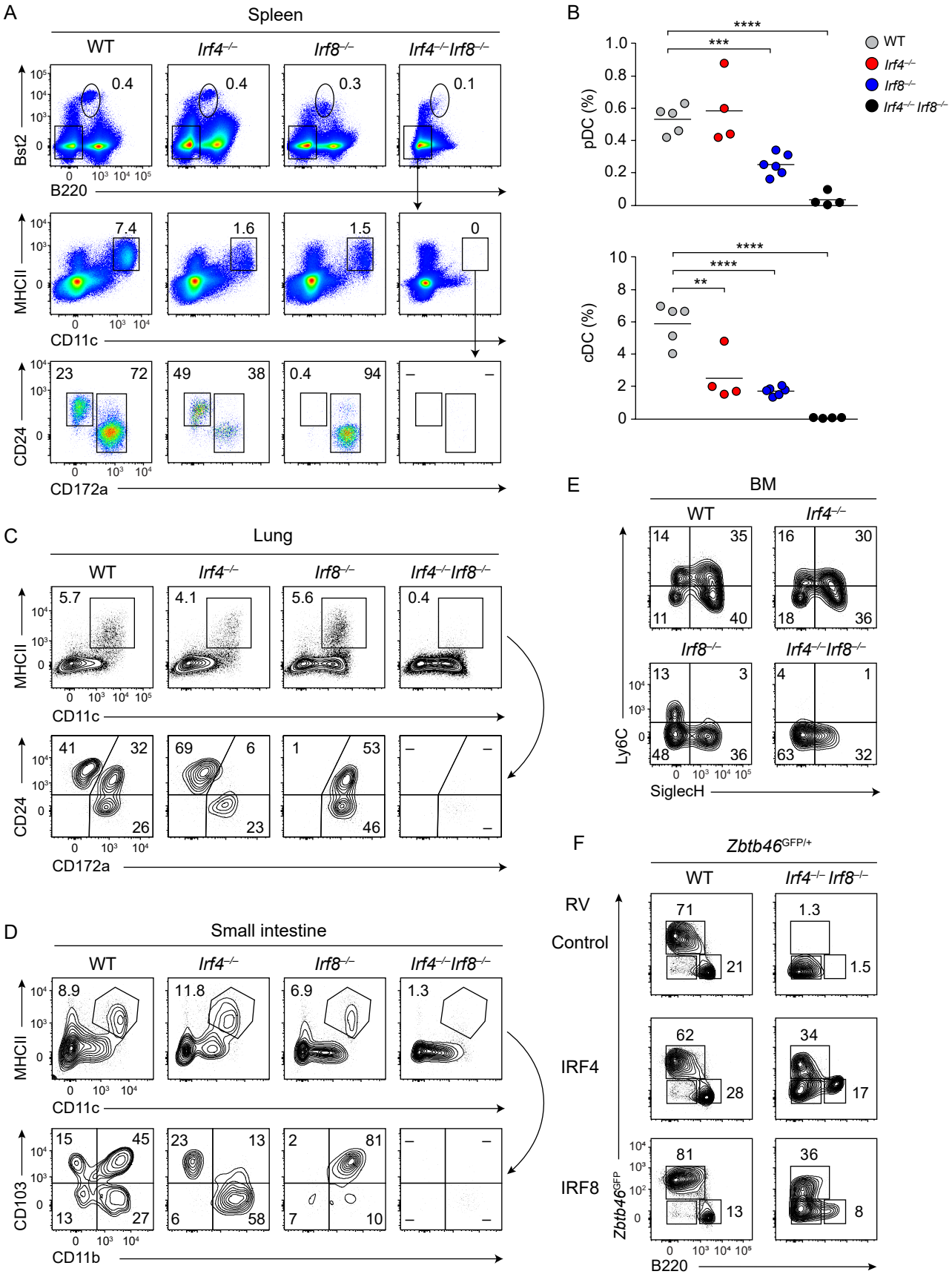
A
Spleen
WT
Irf4−/−
Irf8−/−
Irf4−/−Irf8−/−
Bst2
B220
MHCII
CD11c
CD24
CD172a
B
pDC (%)
cDC (%)
WT
Irf4−/−
Irf8−/−
Irf4−/− Irf8−/−
C
Lung
D
Small intestine
CD103
CD11b
E
BM
Ly6C
SiglecH
F
Zbtb46GFP/+
RV
Control
IRF4
IRF8
Zbtb46GFP
B220

Figure S1. DC analysis in the spleen and peripheral tissues of *Irf4*$^{-/-}$, *Irf8*$^{-/-}$, or *Irf4*$^{-/-}$ *Irf8*$^{-/-}$ mice, related to Figure 1.

(A and B) Analysis of splenic cDCs from WT, *Irf4*$^{-/-}$, *Irf8*$^{-/-}$, and *Irf4*$^{-/-}$ *Irf8*$^{-/-}$ mice. (A) Flow cytometric analysis showing splenic pDC (top), cDC (middle), CD24^{+} CD172a^{-} cDC1, and CD172a^{+} cDC2 (bottom). (B) Scatter plots show the average percentages of pDCs (top) and cDCs (bottom, pre-gate: Bst2^{-} B220^{-} cells) in the splenocytes of the indicated genotypes (bar = average %, n = 4 ~ 5 mice per group). ** P < 0.01, *** P < 0.001, **** P < 0.0001 (Student's t-test). (C and D) Flow cytometric analysis showing cDC in the lung and small intestine lamina propria of the indicated genotypes. Pre-gate: CD45^{+} Ly6C^{-} Ly6G^{-} CD3^{-} B220^{-} cells. Data shown is one of more than three similar analyses. (E) Flow cytometric analysis showing BM progenitor cells from the indicated genotypes. Pre-gate: Lineage^{-} CD11c^{+} MHCII^{-} CD135^{+} CD172a^{-} cells. Data shown is one of three similar experiments. (F) Representative flow cytometric analysis showing *Zbtb46*$^{GFP+}$ cells differentiated from *Zbtb46*$^{GFP/+}$ or *Irf4*$^{-/-}$ *Irf8*$^{-/-}$ *Zbtb46*$^{GFP/+}$ CD117^{hi} BM progenitors retrovirally expressing either *Irf4* or *Irf8*. Data shown is one of two similar analyses. Numbers in the two-color histograms indicate percentages of the gated cells.

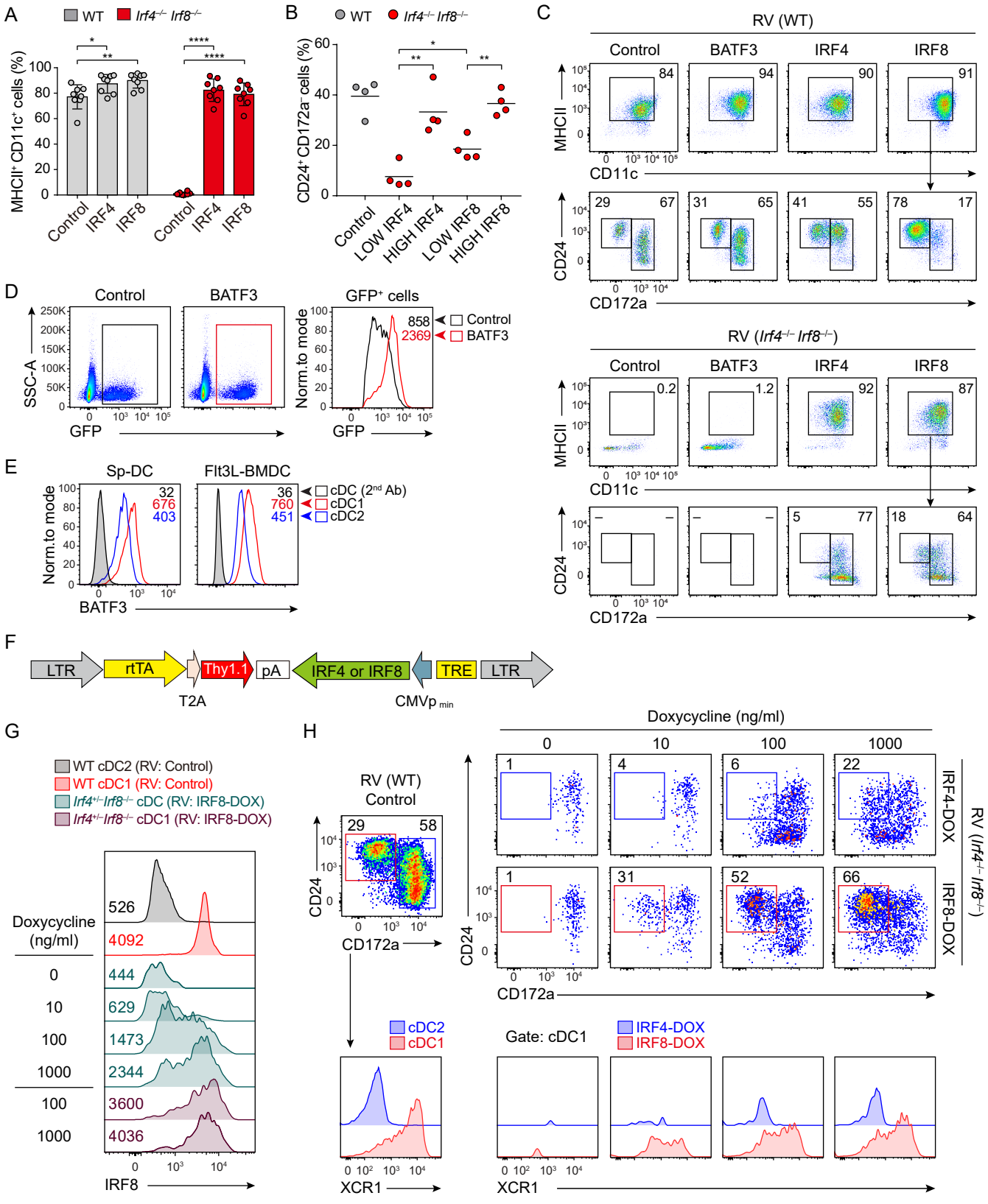
A
WT
Irf4−/− Irf8−/−
MHCII+ CD11c+ cells (%)
Control
IRF4
IRF8
B
CD24+ CD172a− cells (%)
Control
LOW IRF4
HIGH IRF4
LOW IRF8
HIGH IRF8
C
RV (WT)
Control
BATF3
IRF4
IRF8
MHCII
CD11c
CD24
CD172a
RV (Irf4−/− Irf8−/−)
D
Control
BATF3
GFP+ cells
SSC-A
GFP
Norm.to mode
858
2369
E
Sp-DC
Flt3L-BMDC
cDC (2nd Ab)
cDC1
cDC2
BATF3
F
LTR
rtTA
Thy1.1
pA
IRF4 or IRF8
TRE
LTR
T2A
CMVp min
G
WT cDC2 (RV: Control)
WT cDC1 (RV: Control)
Irf4+/−Irf8−/− cDC (RV: IRF8-DOX)
Irf4+/−Irf8−/− cDC1 (RV: IRF8-DOX)
Doxycycline (ng/ml)
0
10
100
1000
100
1000
526
4092
444
629
1473
2344
3600
4036
IRF8
H
RV (WT) Control
CD24
CD172a
cDC2
cDC1
XCR1
Doxycycline (ng/ml)
IRF4-DOX
IRF8-DOX
RV (Irf4−/− Irf8−/−)
Gate: cDC1

Figure S2. Phenotypic analysis of cDCs restored by retroviral *Irf4* or *Irf8*, related to Figure 2.

(A-C) Analysis of cDCs differentiated from WT or *Irf4*$^{-/-}$ *Irf8*$^{-/-}$ CD117^{hi} BM progenitors retrovirally expressing either *Irf4* or *Irf8* without or with *Batf3* co-expression. (A) A bar graph showing average percentages of MHCII^{+} CD11c^{+} cDCs ± SD (*n* = 8), (B) A scatter plot showing the average percentages of CD24^{+} CD172a^{-} cDC1 (bar = average %, *n* = 4) at the indicated conditions. *P < 0.05, ** P < 0.01, **** P < 0.0001 (Student's *t*-test). (C) Flow cytometric analysis showing cDCs differentiated from WT (top) or *Irf4*$^{-/-}$ *Irf8*$^{-/-}$ (bottom) BM progenitors retrovirally expressing *Batf3*, *Irf4*, or *Irf8*. Some of the histogram panels are redundantly shown in Figure 2B. (D) Flow cytometric analysis showing retroviral GFP expression by control RV (black)- or *Batf3* RV (red)-transduced cells. (E) Flow cytometric analysis showing BATF3 expression in the splenic cDCs (left) and BM-derived cDCs (right). (F) A retroviral construct to express IRF4 or IRF8 driven by $CMVp_{min}$ in combination with tetracycline responsive element (TRE) activity. rtTA denotes reverse tetracycline-controlled transactivator. (G and H) Flow cytometric analysis of cDCs differentiated from WT, *Irf4*$^{+/-}$ *Irf8*$^{-/-}$ or *Irf4*$^{-/-}$ *Irf8*$^{-/-}$ BM progenitors retrovirally expressing various amounts of either *Irf4* or *Irf8* by doxycycline treatment (0, 10, 100, or 1000 ng/ml). (G) Expression of IRF8 in the *Irf4*$^{+/-}$ *Irf8*$^{-/-}$ cDC restored at the indicated conditions. (H) Flow cytometric analysis showing cDC1 and cDC2 differentiated from *Irf4*$^{-/-}$ *Irf8*$^{-/-}$ BM progenitors with various amounts of retroviral *Irf4* or *Irf8* achieved by treatment with the indicated concentrations of doxycycline. Single-color histograms below show XCR1 expression on the gated CD24^{+} CD172a^{-} cDC1 under the same conditions. The data shown is one of three similar experiments. Numbers in the single-color and two-color histograms indicate the geometric MFI and the percentage of the gated cells, respectively.

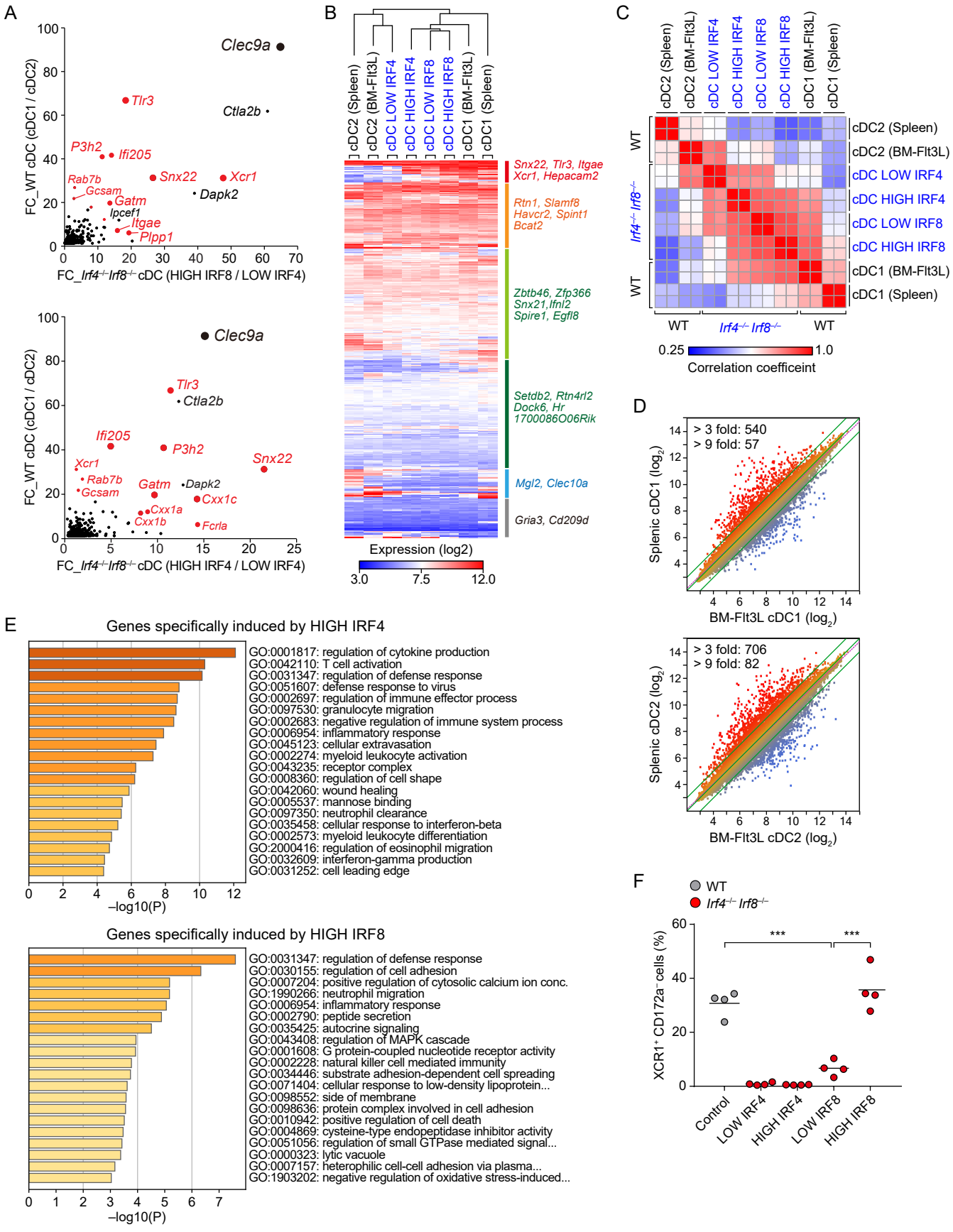
A
FC_WT cDC (cDC1 / cDC2)
FC_Irf4−/− Irf8−/− cDC (HIGH IRF8 / LOW IRF4)
Clec9a
Tlr3
Ctla2b
P3h2
Ifi205
Snx22
Xcr1
Rab7b
Gcsam
Dapk2
Gatm
Ipcef1
Itgae
Plpp1
FC_Irf4−/− Irf8−/− cDC (HIGH IRF4 / LOW IRF4)
Cxx1c
Cxx1a
Cxx1b
Fcrla
B
cDC2 (Spleen)
cDC2 (BM-Flt3L)
cDC LOW IRF4
cDC HIGH IRF4
cDC LOW IRF8
cDC HIGH IRF8
cDC1 (BM-Flt3L)
cDC1 (Spleen)
Snx22, Tlr3, Itgae
Xcr1, Hepacam2
Rtn1, Slamf8
Havcr2, Spint1
Bcat2
Zbtb46, Zfp366
Snx21,Ifnl2
Spire1, Egfl8
Setdb2, Rtn4rl2
Dock6, Hr
1700086O06Rik
Mgl2, Clec10a
Gria3, Cd209d
Expression (log2)
3.0
7.5
12.0
C
WT
Irf4−/− Irf8−/−
0.25
1.0
Correlation coefficeint
D
> 3 fold: 540
> 9 fold: 57
Splenic cDC1 (log2)
BM-Flt3L cDC1 (log2)
> 3 fold: 706
> 9 fold: 82
Splenic cDC2 (log2)
BM-Flt3L cDC2 (log2)
E
Genes specifically induced by HIGH IRF4
GO:0001817: regulation of cytokine production
GO:0042110: T cell activation
GO:0031347: regulation of defense response
GO:0051607: defense response to virus
GO:0002697: regulation of immune effector process
GO:0097530: granulocyte migration
GO:0002683: negative regulation of immune system process
GO:0006954: inflammatory response
GO:0045123: cellular extravasation
GO:0002274: myeloid leukocyte activation
GO:0043235: receptor complex
GO:0008360: regulation of cell shape
GO:0042060: wound healing
GO:0005537: mannose binding
GO:0097350: neutrophil clearance
GO:0035458: cellular response to interferon-beta
GO:0002573: myeloid leukocyte differentiation
GO:2000416: regulation of eosinophil migration
GO:0032609: interferon-gamma production
GO:0031252: cell leading edge
−log10(P)
Genes specifically induced by HIGH IRF8
GO:0031347: regulation of defense response
GO:0030155: regulation of cell adhesion
GO:0007204: positive regulation of cytosolic calcium ion conc.
GO:1990266: neutrophil migration
GO:0006954: inflammatory response
GO:0002790: peptide secretion
GO:0035425: autocrine signaling
GO:0043408: regulation of MAPK cascade
GO:0001608: G protein-coupled nucleotide receptor activity
GO:0002228: natural killer cell mediated immunity
GO:0034446: substrate adhesion-dependent cell spreading
GO:0071404: cellular response to low-density lipoprotein...
GO:0098552: side of membrane
GO:0098636: protein complex involved in cell adhesion
GO:0010942: positive regulation of cell death
GO:0004869: cysteine-type endopeptidase inhibitor activity
GO:0051056: regulation of small GTPase mediated signal...
GO:0000323: lytic vacuole
GO:0007157: heterophilic cell-cell adhesion via plasma...
GO:1903202: negative regulation of oxidative stress-induced...
−log10(P)
F
WT
Irf4−/− Irf8−/−
XCR1+ CD172a− cells (%)
***
***
Control
LOW IRF4
HIGH IRF4
LOW IRF8
HIGH IRF8

Figure S3. Transcriptomic analysis of cDCs restored by retroviral *Irf4* or *Irf8*, related to Figure 3.

(A-D) Microarray analysis of cDCs differentiated from WT or *Irf4*$^{-/-}$ *Irf8*$^{-/-}$ CD117^{hi} BM progenitors retrovirally expressing either *Irf4* or *Irf8* without or with *Batf3* co-expression. (A) Scatter plots showing the top 3000 genes with > 2-fold expression in cDC1 compared to cDC2. Axes depict fold change ratios (FC) of cDC1 to cDC2 from WT mice (y-axis) compared against those of high IRF8 to low IRF4 conditions (x-axis, top) or of high IRF4 to low IRF4 (x-axis, bottom) of *Irf4*$^{-/-}$ *Irf8*$^{-/-}$ mice. cDC1-specific genes are highlighted in red. (B and C) Heatmap and Spearman's rank correlation coefficient showing the expression of 462 DC-specific genes (log_2 values) in WT cDCs (black) and *Irf4*$^{-/-}$ *Irf8*$^{-/-}$ cDCs (blue) differentiated at the indicated conditions. (D) Scatter plots comparing gene expressions between splenic cDC and BM-derived cDC differentiated with Flt3L (top: cDC1 and bottom: cDC2). (E) Gene pathway analysis for the genes specifically controlled by either *Irf4* or *Irf8* using Metascape platform. (F) A scatter plot showing the average percentages of XCR1^{+} CD172a^{-} cDC1 (bar = average %, n = 4) differentiated from WT or *Irf4*$^{-/-}$ *Irf8*$^{-/-}$ BM progenitors at the indicated conditions. *** $P < 0.001$ (Student's t-test).

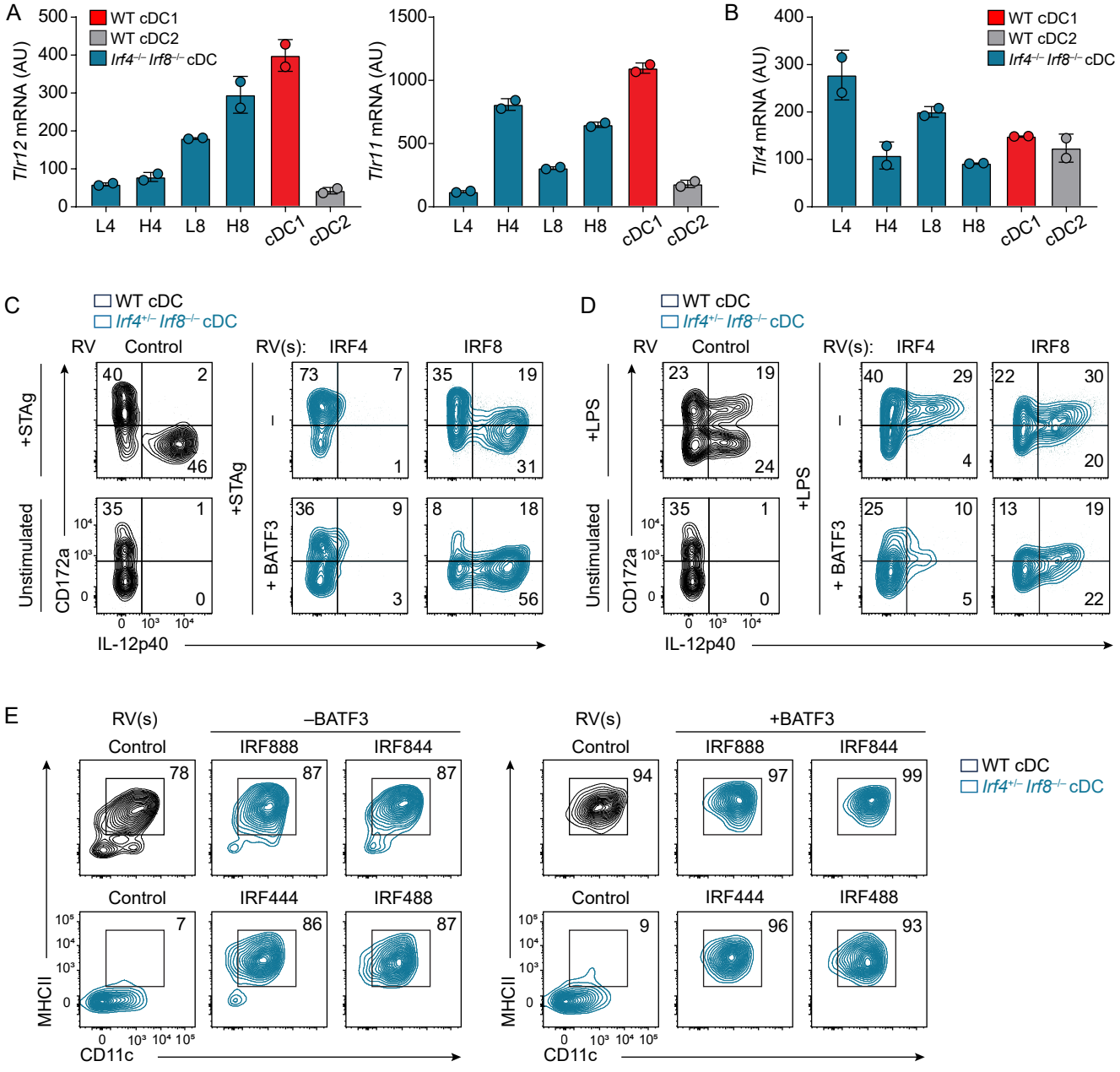
A
WT cDC1
WT cDC2
Irf4−/− Irf8−/− cDC
Tlr12 mRNA (AU)
Tlr11 mRNA (AU)
L4
H4
L8
H8
cDC1
cDC2
B
Tlr4 mRNA (AU)
C
WT cDC
Irf4+/− Irf8−/− cDC
RV
Control
RV(s):
IRF4
IRF8
+STAg
Unstimulated
+ BATF3
CD172a
IL-12p40
D
+LPS
E
RV(s)
–BATF3
+BATF3
Control
IRF888
IRF844
IRF444
IRF488
MHCII
CD11c

Figure S4. Phenotypic and functional analysis of cDCs restored by retroviral *Irf4*, *Irf8*, or *Irf4-Irf8* chimeras, related to Figure 3.

(A-E) Analysis of cDCs differentiated from WT, *Irf4*$^{+/-}$ *Irf8*$^{-/-}$, or *Irf4*$^{-/-}$ *Irf8*$^{-/-}$ CD117^{hi} BM progenitors retrovirally expressing either *Irf4* or *Irf8* without or with *Batf3* co-expression. (A and B) Microarray analysis showing mRNA expression of *Tlr12*, *Tlr11*, and *Tlr4* in the cDCs restored at the indicated conditions. L4 (LOW IRF4), H4 (HIGH IRF4), L8 (LOW IRF8), and H8 (HIGH IRF8). (C and D) Flow cytometric analysis showing IL-12 p40 production from the restored cDCs upon stimulation with either STAg (1 μg/ml) or *E. coli* LPS (1 μg/ml) for 6 h. Data shown is one of three similar experiments. (E) Flow cytometric analysis showing CD11c^{+} MHCII^{+} cDCs differentiated from *Irf4*$^{+/-}$ *Irf8*$^{-/-}$ BM progenitors expressed with retroviral *Irf4* (IRF444), *Irf8* (IRF888) or *Irf4-Irf8* chimeras (IRF488 or IRF844) without or with *Batf3* co-expression. Data shown is one of three similar experiments.

A Peaks shared by IRF4 and BATF3 (cDC2), # Tg seq. = 643

Motif	*P*-value	% Tg/Bg	Best match
	1e-260	61/7.6	PU.1 or SpiB
	1e-117	37/6.2	AP-1
	1e-102	13/0.3	AP-1-IRF
	1e-45	22/5.3	RUNX

B LOW IRF4 vs. HIGH IRF4
198 genes (HIGH IRF4 > LOW IRF4, > 2 fold)
IRF8 ChIP-seq for cDC1: # Tg seq. = 326

Motif	*P*-value	% Tg/Bg	Best match
	1e-100	51/7.0	PU.1-IRF
	1e-59	37/6.1	PU.1 or SpiB
	1e-26	12/1.2	AP-1-IRF
	1e-13	15/4.1	ZNF
	1e-13	2.5/0	PU.1 or SpiB

* cDC differentiated from *Irf4*$^{-/-}$*Irf8*$^{-/-}$ BM progenitors

C HIGH IRF4 vs. HIGH IRF8
190 genes (HIGH IRF8 > HIGH IRF4, > 2 fold)
IRF8 ChIP-seq for cDC1: # Tg seq. = 474

Motif	*P*-value	% Tg/Bg	Best match
	1e-176	52/5.7	PU.1-IRF
	1e-58	18/1.8	PU.1 or SpiB
	1e-33	10/0.9	AP-1-IRF
	1e-17	11/2.4	AP1
	1e-15	9.9/2.4	RUNX

* cDC differentiated from *Irf4*$^{-/-}$*Irf8*$^{-/-}$ BM progenitors

D

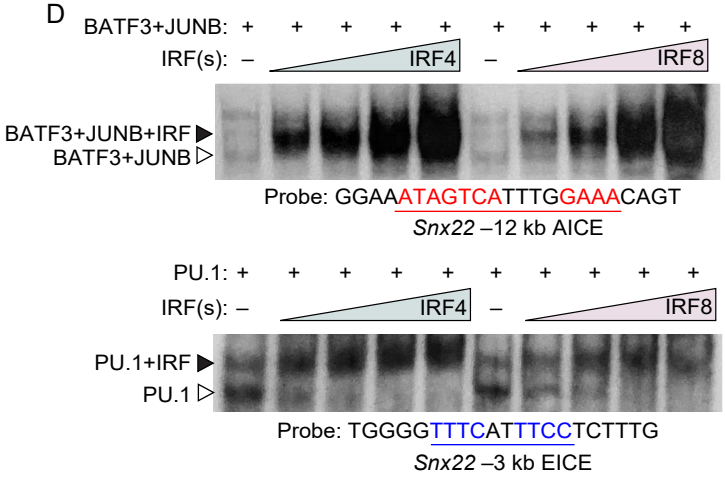

E

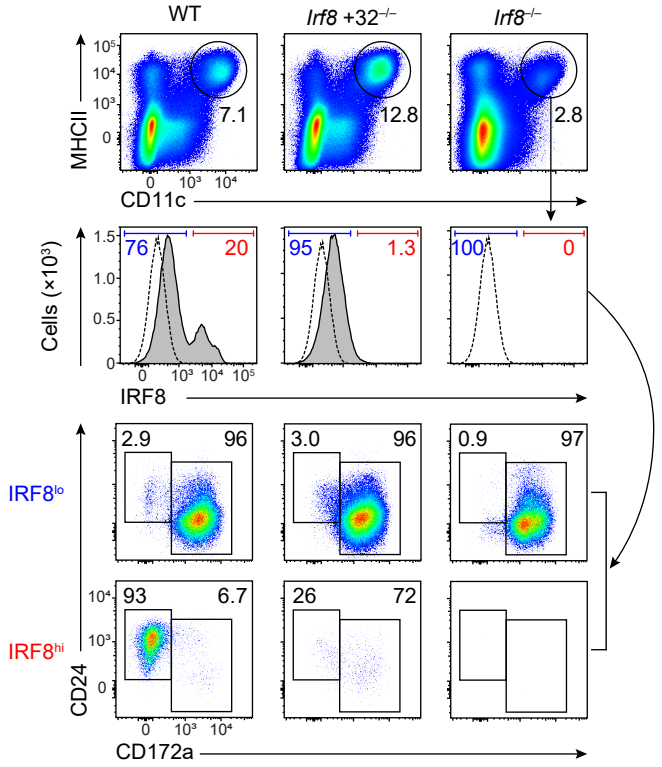

Figure S5. High amounts of IRF4 bind AICE, related to Figure 5.

(A) *De novo* motif analysis for ChIP-seq peaks shared by IRF4 and BATF3 in cDC2. (B and C) *De novo* DNA motifs for IRF8 ChIP-seq peaks merged with (B) 198 increased genes (> 2 fold) at high IRF4 condition compared to low IRF4 condition, or (C) 190 increased genes (> 2 fold) at high IRF8 condition compared to high IRF4 condition. Differentially expressed gene sets between the compared conditions were selected based on microarray analysis of *Irf4*$^{-/-}$ *Irf8*$^{-/-}$cDCs restored by retroviral *Irf4* or *Irf8* without or with *Batf3* co-expression (Table S1). Genomic regions selected for motif analysis: gene body ± 50 kb. # Tg seq. and % Tg/Bg denote the number of total target sequences and percentage of target/percentage of background sequence, respectively. (D) EMSA showing bindings of either IRF4 or IRF8 to DNA containing AICE (top) or EICE (bottom). Probe sequences containing AICE (*Snx22* –12 kb, AICE: red) or EICE (*Snx22* –3 kb, EICE: blue) are indicated below each of the gels. (E) Flow cytometric analysis showing IRF8 expression in splenic cDC of the indicated genotypes (top and second from the top). Pre-gate: CD64^{-} B220^{-} cells. Two-color histograms at the bottom show the proportions of cDC1 and cDC2 in the IRF8^{lo} (second from the bottom) and IRF8^{hi} (bottom) cDC populations. Numbers in the histograms are the percentages of the gated cells.

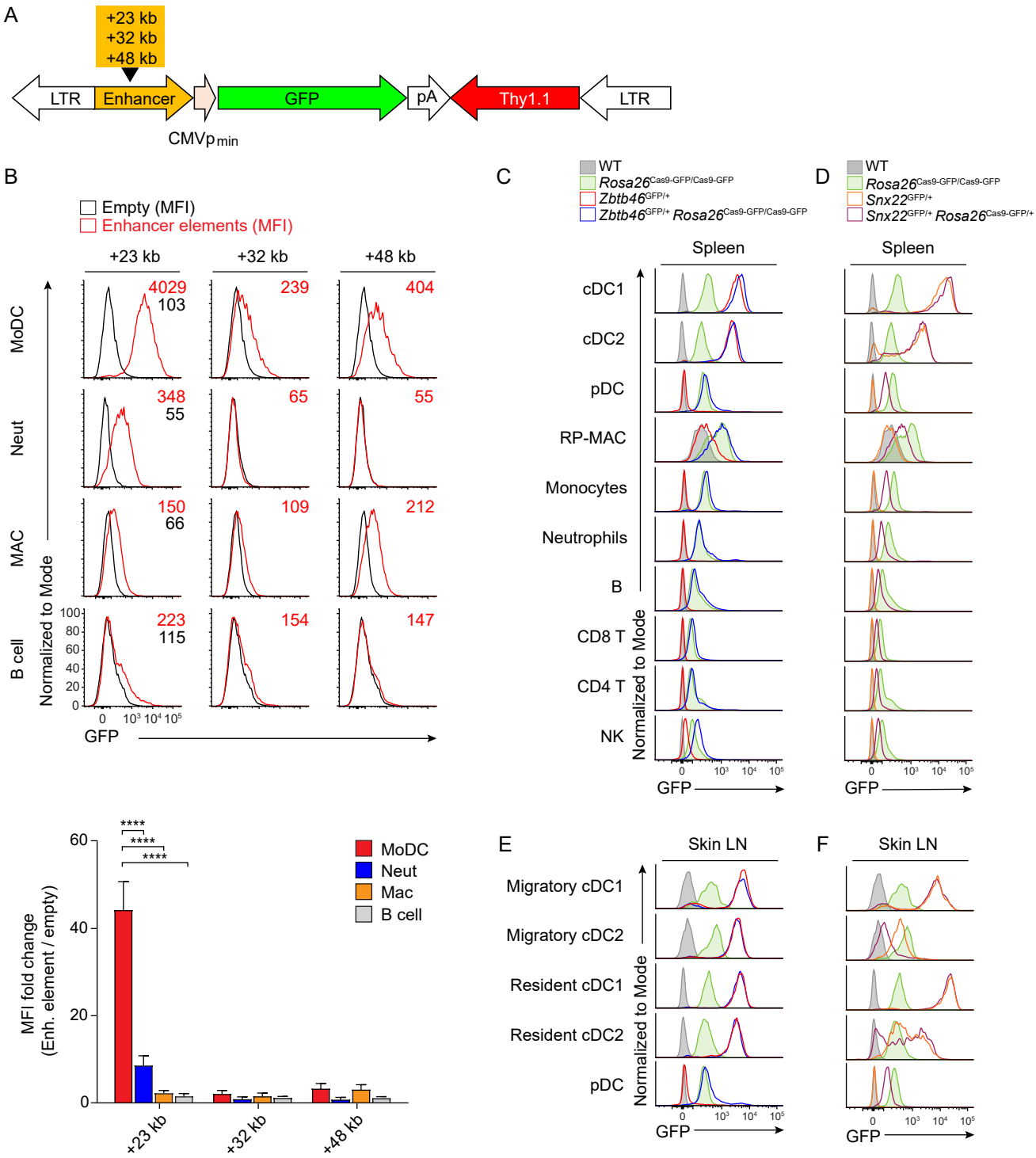
A
+23 kb
+32 kb
+48 kb
LTR
Enhancer
GFP
pA
Thy1.1
LTR
CMVp min
B
Empty (MFI)
Enhancer elements (MFI)
+23 kb
+32 kb
+48 kb
MoDC
Neut
MAC
B cell
4029
103
239
404
348
55
65
55
150
66
109
212
223
115
154
147
Normalized to Mode
GFP
C
WT
Rosa26Cas9-GFP/Cas9-GFP
Zbtb46GFP/+
Zbtb46GFP/+ Rosa26Cas9-GFP/Cas9-GFP
Spleen
cDC1
cDC2
pDC
RP-MAC
Monocytes
Neutrophils
B
CD8 T
CD4 T
NK
Normalized to Mode
GFP
D
WT
Rosa26Cas9-GFP/Cas9-GFP
Snx22GFP/+
Snx22GFP/+ Rosa26Cas9-GFP/+
Spleen
GFP
MFI fold change
(Enh. element / empty)
****
****
****
MoDC
Neut
Mac
B cell
+23 kb
+32 kb
+48 kb
E
Skin LN
Migratory cDC1
Migratory cDC2
Resident cDC1
Resident cDC2
pDC
Normalized to Mode
GFP
F
Skin LN
GFP

Figure S6. Transcriptional activity of *Zbtb46* enhancer elements and expression of *Zbtb46*^{GFP} or *Snx22*^{GFP} in various immune cells, related to Figures 6 and 7.

(A) A retroviral construct to assess integrated GFP-reporter activity driven by $CMVp_{min}$ in combination with various enhancer elements. (B) Flow cytometric analysis for GFP-reporter activities in MoDC, neutrophils (Neut), macrophages (MAC), or splenic B cells transduced with empty retrovirus (black) or retroviruses expressing *Zbtb46* +23 kb, +32 kb, or +48 kb elements (red). Culture methods for each cell type are described in the 'experimental model and subject details' section of the STAR METHODS. A bar graph below shows average MFI fold changes (MFI of enhancer element / MFI of empty) ± SD for each cell type ($n = 4$). **** $P < 0.0001$ (Student's *t*-test). (C-F) Flow cytometric analysis showing GFP expression of various immune cells in the (C and D) spleen or (E and F) skin-draining lymph nodes from mice of the indicated genotypes. Gating strategies to identify the indicated cell types are as followings: (i) in the spleen, cDC pre-gate: F4/80$^-$ Bst2$^-$ B220$^-$ CD11c$^+$ MHCII$^+$ cells, cDC1: CD24$^+$ CD172a$^-$ cells, cDC2: CD172a$^+$ cells, pDC: F4/80$^-$ Bst2$^+$ B220$^+$ cells, red pulp macrophages (RP-MAC): F4/80$^+$ CD64$^+$ MHCII^{int} CD11c^{int} cells, monocytes: B220$^-$ CD11b$^+$ Ly6C^{hi} Ly6G$^-$ cells, neutrophils: B220$^-$ CD11b$^+$ Ly6C^{int} Ly6G$^+$ cells, B cells: B220$^+$ MHCII$^+$ cells, CD4$^+$ T cells: B220$^-$ CD3$^+$ CD4$^+$ cells, CD8$^+$ T cells: B220$^-$ CD3$^+$ CD8$^+$ cells, and NK cells: B220$^-$ NK1.1$^+$ cells, (ii) in the skin lymph nodes, cDC pre-gate: F4/80$^-$ Bst2$^-$ B220$^-$ EpCAM$^-$ cells, migratory cDC1: MHCII^{hi} CD11c$^+$ CD24$^+$ CD172a$^-$ cells, migratory cDC2: MHCII^{hi} CD11c$^+$ CD172a$^+$ cells, resident cDC1: MHCII^{int} CD11c$^+$ CD24$^+$ CD172a$^-$ cells, resident cDC2: MHCII^{int} CD11c$^+$ CD172a$^+$ cells, and pDC: F4/80$^-$ Bst2$^+$ B220$^+$ cells.

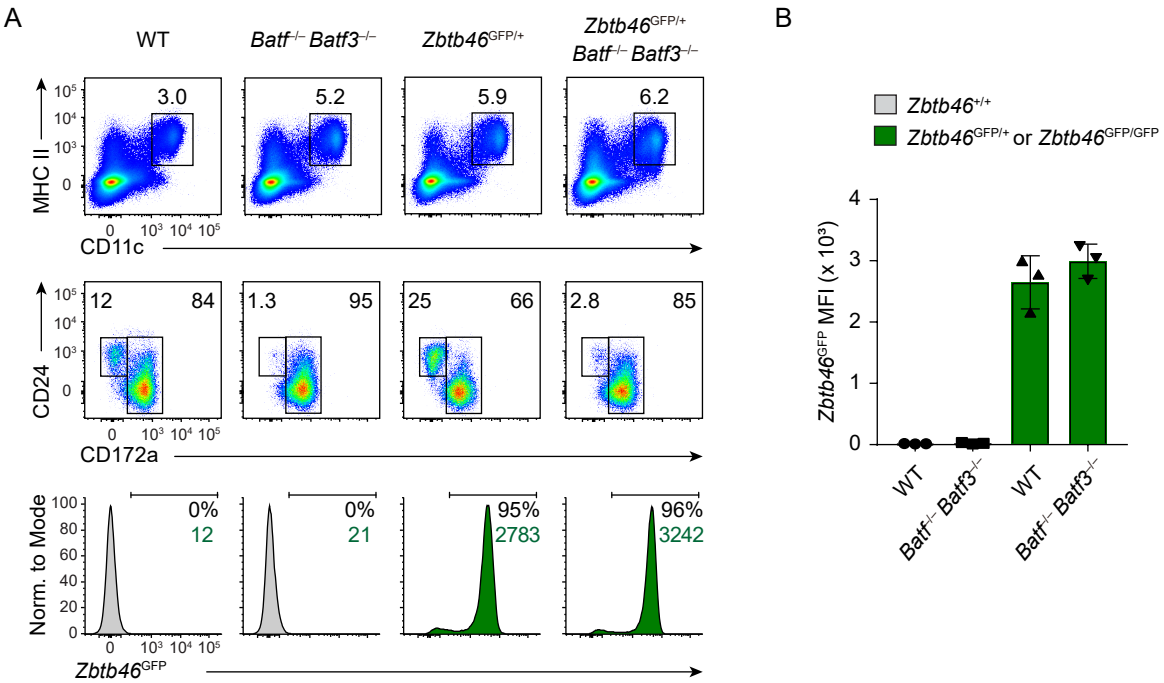
A
WT
Batf−/− Batf3−/−
Zbtb46GFP/+
Zbtb46GFP/+ Batf−/− Batf3−/−
MHC II
CD11c
3.0
5.2
5.9
6.2
CD24
CD172a
12
84
1.3
95
25
66
2.8
85
Norm. to Mode
Zbtb46GFP
0%
12
0%
21
95%
2783
96%
3242
B
Zbtb46+/+
Zbtb46GFP/+ or Zbtb46GFP/GFP
Zbtb46GFP MFI (x 10³)
WT
Batf−/− Batf3−/−
WT
Batf−/− Batf3−/−

Figure S7. *Batf*$^{-/-}$ *Batf3*$^{-/-}$ cDC2 normally express *Zbtb46*^{GFP}, related to Figure 6.

(A) Flow cytometric analysis showing *Zbtb46*^{GFP}expression in the splenic cDC2 from mice of the indicated genotypes. Numbers in the two-color histograms indicate the percentage of the gated cells (top and middle). Numbers in the single-color histograms (bottom) indicate *Zbtb46*$^{GFP+}$ cell percentage (upper, black) and geometric MFI of the cells (lower, green). (B) A bar graph shows the average geometric MFI ± SD (*n* = 3).